Vapor–Liquid Equilibria of Mixtures Containing Alkanes, Carbon Dioxide, and Nitrogen

Jeffrey J. Potoff and J. Ilja Siepmann
Dept. of Chemistry and Dept. of Chemical Engineering and Materials, University of Minnesota, Minneapolis, MN 55455

New force fields for carbon dioxide and nitrogen are introduced that quantitatively reproduce the vapor–liquid equilibria (VLE) of the neat systems and their mixtures with alkanes. In addition to the usual VLE calculations for pure CO_2 and N_2, calculations of the binary mixtures with propane were used in the force-field development to achieve a good balance between dispersive and electrostatic (quadrupole–quadrupole) interactions. The transferability of the force fields was then assessed from calculations of the VLE for the binary mixtures with n-hexane, the binary mixture of CO_2/N_2, and the ternary mixture of CO_2/N_2/propane. The VLE calculations were carried out using configurational-bias Monte Carlo simulations in either the grand canonical ensemble with histogram–reweighting or in the Gibbs ensemble.

Introduction

The design of separation processes requires accurate knowledge of the vapor–liquid equilibria for each of the pure components and the multicomponent mixture. Of particular interest is the phase behavior of mixtures containing alkanes, CO_2 and N_2, which are typically found in the petrochemical industry. One example is the flooding of petroleum reservoirs with CO_2 or N_2 to enhance oil recovery. Furthermore, significant effort has been expended designing chemical processes where supercritical CO_2 is used as a "green"solvent (Brunner, 1994; Mishima et al., 2000). This is due to the fact that CO_2 has nearly ideal physical properties for such applications, including a low critical temperature of 304.3 K and moderate critical pressure of 73.8 bar (Rainwater, 1991).

Calculations of vapor–liquid equilibria (VLE) in chemical engineering have traditionally been performed with an equation of state (EOS) (Reid et al., 1977). These EOS models are based on pure-phase properties, are easy to use, and require little computational effort, but often yield only qualitative predictions of binary and ternary mixture VLE. For a quantitative representation of the VLE, however, it is usually necessary to introduce empirically derived binary interaction parameters. This need for binary interaction parameters tends to limit the predictive capability of EOS models to systems where experimental data are readily available.

Another promising alternative to EOS models for VLE calculations is molecular simulation. Over the last 10 years, the introduction of new simulation methodologies, such as Gibbs ensemble Monte Carlo (GEMC) (Panagiotopoulos, 1987; Panagiotopoulos et al., 1988), a recent molecular dynamics variant of GEMC (Baranyai and Cummings, 2000), histogram-reweighting techniques (Ferrenberg and Swendsen, 1988, 1989), and Gibbs-Duhem integration (Kofke, 1992), have made the calculation of phase equilibria from simulation a routine task. If an accurate and transferable force field is available, then molecular simulations have an advantage over EOS calculations in terms of their predictive capability, which comes at the expense of a significantly higher expenditure of computer time necessary to determine a coexistence curve.

In this work, we demonstrate how molecular simulation techniques can be used to develop transferable force fields and to predict the VLE of binary and ternary mixtures of substances relevant to common industrial processes. We focus our attention on mixtures of nonpolar and (slightly) polar molecules. The accurate prediction of VLE for these systems has until now been possible only by fitting system-specific binary interaction parameters (Liu and Beck, 1998) or by using special combining rules for unlike-pair interactions on differ-

---

Correspondence concerning this article should be addressed to J. I. Siepmann.
Permanent address of J. J. Potoff: Dept. of Chemical Engineering and Materials Science, Wayne State University, 5050 Anthony Wayne Drive, Detroit, MI 48202.

ent molecules (Potoff et al., 1999), that is the Lorentz-Berthelot combining rules (Maitland et al., 1981) were used for unlike interactions of atoms belonging to the same type of molecule (such as methyl and methylene groups on propane), whereas the Kong combining rules (Kong, 1973; Maitland et al., 1981) were used for unlike-pair interactions of molecules of different types (such as methyl group in propane and oxygen atom in CO_2). Use of different combining rules within the same system is not entirely consistent and limits the transferability of the force fields. The force field employed in this work is the nonpolarizable all-atom transferable potentials for phase equilibria (TraPPE) force field, which makes use of Lennard-Jones potentials for the overlap and dispersive interactions, while simple point charges are used for the first-order electrostatic and induction interactions (Maitland et al., 1981). The Lennard-Jones parameters for *all* unlike-pair interactions (irrespective of whether the sites belong to molecules of the same type or of different types) are determined from the commonly used Lorentz-Berthelot combining rules (Allen and Tildesley, 1987). Configurational-bias histogram-reweighting Monte Carlo simulations in the grand canonical ensemble were used to calculate pure-component phase diagrams for CO_2 and N_2 and the phase diagrams for the binary mixtures CO_2/propane, CO_2/n-hexane, CO_2/N_2, and N_2/propane. Gibbs ensemble Monte Carlo was used for VLE calculations of the ternary mixture CO_2/N_2/propane.

The remainder of this article is organized as follows. In the next section, the force fields used in this work are described in detail. The computational details of this work are listed in the third section. The results of our simulations are presented and discussed in the fourth section. Comparisons are made between our newly developed models for CO_2 and N_2 and others found in the literature. The conclusions of our work are given in the fifth section.

Models

Alkanes

The TraPPE-EH force field (Chen and Siepmann, 1999), which is based on an explicit-hydrogen representation, is used for propane and n-hexane. Nonbonded interaction sites interact via a pairwise-additive Lennard-Jones 12-6 potential

$$U(r_{ij}) = 4\epsilon_{ij}\left[\left(\frac{\sigma_{ij}}{r_{ij}}\right)^{12} - \left(\frac{\sigma_{ij}}{r_{ij}}\right)^{6}\right], \tag{1}$$

where r_{ij}, ϵ_{ij}, and σ_{ij} are the separation, LJ well depth, and LJ size, respectively, for the pair of atoms i and j. The LJ parameters for interactions between like atoms are listed in Table 1. The parameters for unlike-pair interactions are calculated with the Lorentz-Berthelot combining rules that are commonly used in molecular simulations (Allen and Tildesley, 1987)

$$\sigma_{ij} = (\sigma_{ii} + \sigma_{jj})/2 \tag{2}$$

$$\epsilon_{ij} = \sqrt{\epsilon_{ii}\epsilon_{jj}}\,. \tag{3}$$

C–C sites are separated by 1.54 Å, a value close to the experimental bond length for long alkanes. Hydrogen interaction sites are placed at the midpoint of the C–H bonds (0.55 Å away from the C site), which were found to yield a better representation of the alkanes than H sites at the H nuclei (Chen and Siepmann, 1999). Intramolecular flexibility is governed by bond angle bending and torsional potentials (Chen and Siepmann, 1999).

Table 1. Lennard-Jones Parameters and Partial Charges for the TraPPE Force Field

Site	ϵ/k_b [K]	σ [Å]	q [e]
C–H	15.3	3.31	0.0
C (in alkane CH_3 group)	4.0	3.30	0.0
C (in alkane CH_2 group)	5.0	3.65	0.0
C (in CO_2)	27.0	2.80	+0.70
O (in CO_2)	79.0	3.05	−0.35
N (in N_2)	36.0	3.31	−0.482
COM (in N_2)	0.0	0.0	+0.964

Carbon dioxide

There have been a number of models proposed for CO_2 (Murthy et al., 1983; Harris and Yung, 1995; Vrabec and Fischer, 1997; Potoff et al., 1999). However, only the EMP2 model by Harris and Yung (1995) and its exp-6 variant (Potoff et al., 1999) were optimized for VLE calculations. While both the LJ and exp-6 forms of the EMP2 force field yield accurate pure-component VLE data, only a qualitative representation of the binary mixture phase diagram for n-alkane/CO_2 mixtures is possible unless special combining rules are used for the unlike-pair interactions (Potoff et al., 1999). To rectify this, we have developed our own CO_2 force field that is consistent with the TraPPE-EH model for n-alkanes. This model has three Lennard-Jones sites that model the overlap and dispersion forces (Maitland et al., 1981). Partial point charges are centered at each LJ site to approximate the first-order electrostatic and second-order induction interactions (Maitland et al., 1981). The C–O bond length and O–C–O bond angle are fixed at the experimental value of 1.16 Å and at 180°, respectively. Tests of a model with a flexible bond angle showed that the flexible and rigid models yield indistinguishable phase equilibrium properties. The parameter set for the TraPPE CO_2 force field is listed in Table 1.

Nitrogen

As in the case of CO_2, a number of intermolecular force fields for N_2 can be found in the literature (Murthy et al., 1983; Galassi and Tildesley, 1994). None of these force fields were optimized for VLE calculations, which is the motivation behind the development of the TraPPE N_2 force field. This force field consists of three sites. Each nitrogen atom is modeled by a Lennard-Jones site separated by the experimental bond length of 1.10 Å. The Lennard-Jones parameters for these sites are listed in Table 1. The gas-phase quadrupole moment of N_2 ($Q = -1.4\times10^{-26}$ esu) (Gray and Gubbins, 1984) was reproduced by placing point charges of $-0.482\ e$ on each Lennard-Jones site. To maintain charge neutrality, a point charge of $+0.964\ e$ was placed at the center of mass (COM) of the N_2 molecule.

Simulation details

Pure component and binary mixtures

Pure-component and binary-mixture phase diagrams were calculated from grand canonical histogram-reweighting Monte Carlo simulations. The application of histogram-reweighting methods to binary mixture VLE calculations is described in detail in the original references and is not repeated here (Potoff and Panagiotopoulos, 1998; Potoff et al., 1999). The Monte Carlo program employs rigid molecule translations and rotations, conformational changes for the semiflexible alkanes, and molecule insertions and removals. The coupled–decoupled configurational-bias Monte Carlo method (Martin and Siepmann, 1999) was used for the latter three types of moves. Lennard-Jones interactions were truncated at 10 Å, and analytical long-range corrections were applied to the energy, pressure, and chemical potential (Allen and Tildesley, 1987). Electrostatic interactions were calculated with the Ewald summation technique using tinfoil boundary conditions, an Ewald screening parameter $\kappa \times L = 5$, and $K_{max} = 5$ for the upper bound of the reciprocal space summation (Allen and Tildesley, 1987).

Pure-component simulations used a box length of $L = 20$ Å (or 25 Å near the critical region), while $L = 25$ Å was used for the binary-mixture calculations. Critical points for the binary mixtures were determined via a mixed-field analysis (Bruce and Wilding, 1992; Potoff and Panagiotopoulos, 1998) using a system size of $L = 25$ Å, except for the CO_2/*n*-hexane mixture, where $L = 30$ Å. The critical parameters reported here are estimates for a single system size. To obtain more precise values of the critical parameters would require additional and longer simulations for larger system sizes (Wilding, 1995; Potoff and Panagiotopoulos, 1998). The final configuration of a previous run was used as the initial configuration for another simulation at a different state point. Equilibration periods of more than 10^6 Monte Carlo steps (MCS) were used. Away from the critical region, vapor-phase simulations were run for 5×10^6 MCS, while simulations in the liquid phase were run for 1 to 2×10^7 MCS. The production periods were lengthened to 5×10^7 MCS in the critical region. Simulation data were stored in the form of lists containing the number of molecules of each species and the energy of the system. Samples were written to this list every 250 or 500 MCS.

Ternary mixtures

The GEMC technique (Panagiotopoulos, 1987; Panagiotopoulos et al., 1988) was used to determine the phase behavior of the ternary mixture CO_2/N_2/propane. The more direct GEMC technique avoids the need to construct a free-energy surface over four-dimensional space, which would have been required if the histogram-reweighting techniques had been used. While not impossible, histogram-reweighting tends to become cumbersome to apply to systems of three or more components at conditions far from criticality.

The GEMC simulations were performed for $N = 150$ molecules. Equilibration periods of 10^4 MC cycles (N attempted MC moves per cycle) were used and results were averaged over the next 5×10^4 MC cycles. As in the grand canonical Monte Carlo simulations, Lennard-Jones interactions were truncated at 10 Å with the appropriate long-range corrections applied, and the electrostatic interactions were calculated via an Ewald summation technique with the same parameters.

Results

Pure components

We present two models for CO_2. The first is a minor variation of the EMP2 force field where parameters for the LJ well depth and collision diameter were shifted slightly to compensate for a change in the C–O bond length. In the original model by Harris and Yung (1995), an effective bond length of 1.149 Å was used, while the experimental bond length of 1.16 Å was used in this work to maintain consistency between this model and the TraPPE models for the *n*-alkanes and nitrogen. The second model for CO_2 is an alternate parameterization derived by us (TraPPE CO_2). In particular, the Lennard-Jones parameters and partial charges were optimized to reproduce the vapor–liquid phase diagram of the binary mixture of CO_2/propane. Thus, propane is essentially used as a "probe" molecule to find a suitable balance of the Lennard-Jones (overlap and dispersive) and Coulombic (first-order electrostatic and induction) interactions. It should be noted, that this approach treats the interactions as effective interactions, that is, the Lennard-Jones r^{-6} part implicitly includes many-body dispersive interactions and the additional contributions arising from instantaneous dipole–quadrupole (r^{-8}) and quadrupole–quadrupole (r^{-10}) interactions. In a similar way, the partial charges mimic both the first-order electrostatic and second-order induction forces, and the TraPPE CO_2 quadrupole moment ($Q = -4.52 \times 10^{-26}$esu) is slightly enhanced compared to the experimental value for an isolated CO_2 molecule ($Q = -4.4 \times 10^{-26}$esu) (Gray and Gubbins, 1984), but remains within the statistical uncertainty of the experimental measurement.

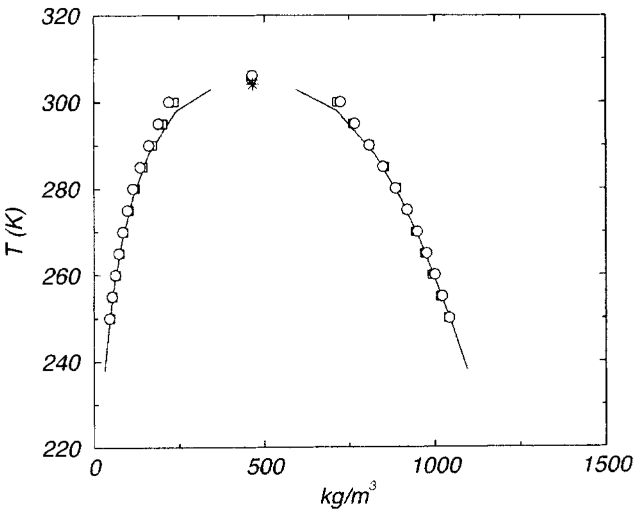

Figure 1. Vapor–liquid coexistence curve for carbon dioxide.

Experimental coexistence data and critical point (solid line and asterisk) (NIST, 2000), EMP2 model (squares), and TraPPE model (circles); statistical uncertainties are smaller than the symbol sizes.

Much larger enhancements are a common feature for molecular models that were fitted to describe the liquid state of dipolar fluids, for example, water (Jorgensen, 1983).

The performance of these models with respect to the prediction of vapor–liquid coexistence densities is compared in Figure 1. Both models yield an equally accurate representation of the phase diagram for neat CO_2. The vapor pressure as a function of temperature is shown in Figure 2. Again, both models predict the vapor pressure of CO_2 over the temperature range of interest equally well. The estimated critical parameters for the TraPPE and modified EMP2 CO_2 models are $T_c = 306.2$ K, $P_c = 77.7$ bar, $\rho_c = 464.9$ kg/m^3 and $T_c = 305.5$ K, $P_c = 76.9$ bar, $\rho_c = 462.5$ kg/m^3, respectively. Thus both models yield excellent agreement with the experimental data (Moldover and Gallagher, 1978; NIST, 2000): $T_c = 304.21$ K, $P_c = 73.843$ bar, and $\rho_c = 466.50$ kg/m^3.

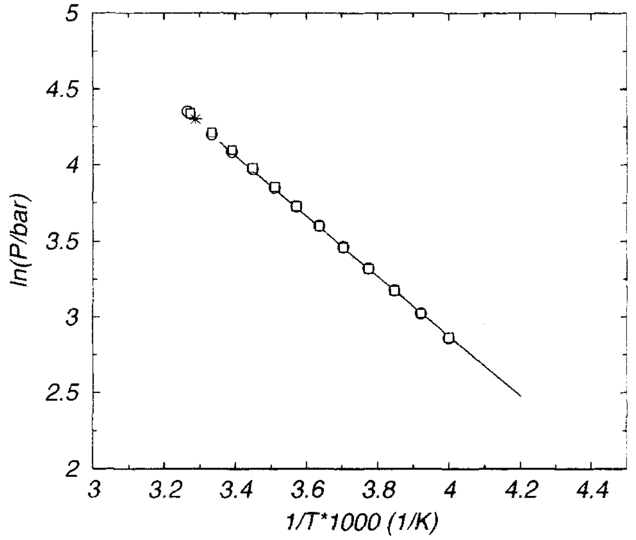

Figure 2. Clausius-Clapeyron plot of the saturated vapor pressure for carbon dioxide vs. the inverse temperature.

Experimental data and critical point (solid line and asterisk) (NIST, 2000), EMP2 model (squares), and TraPPE model (circles).

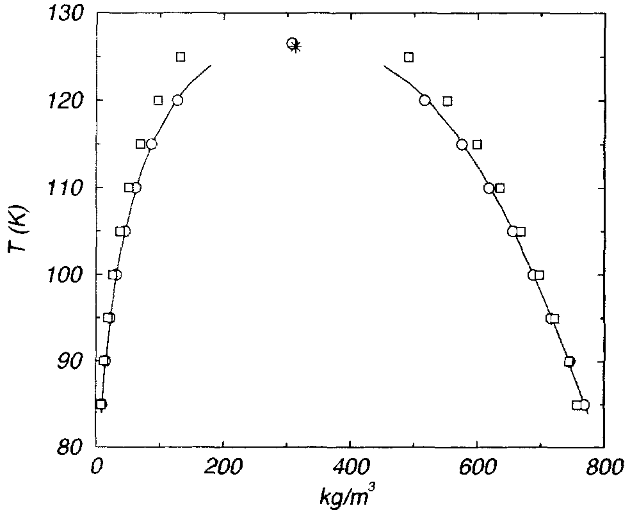

Figure 3. Vapor–liquid coexistence curve for nitrogen.

Experimental coexistence data and critical point (solid line and asterisk) (NIST, 2000), GT model (squares), and TraPPE model (circles).

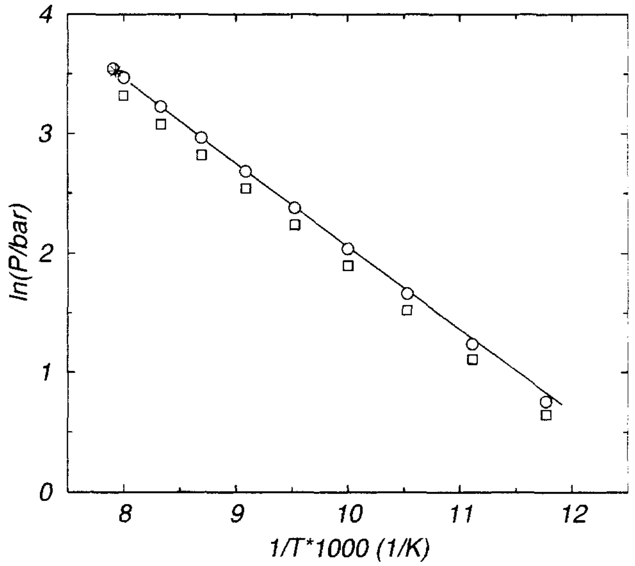

Figure 4. Clausius-Clapeyron plot of the saturated vapor pressure for nitrogen vs. the inverse temperature.

Experimental data and critical point (solid line and asterisk) (NIST, 2000), GT model (squares), and TraPPE model (circles).

In Figure 3, the vapor–liquid coexistence curves of N_2 for the TraPPE model and the GT model of Galassi and Tildesley (1994) are shown. The TraPPE force field for N_2 is in good agreement with experimental data (NIST, 2000) with respect to the saturated liquid and vapor densities over the entire temperature range of interest. In contrast, the GT model underpredicts the saturated vapor densities. As a result, the vapor pressure, shown in Figure 4, of the GT model is approximately 15% too low over the entire temperature range of interest. The TraPPE force field gives vapor pressures that are in close agreement with experimental data from 85 K to 125 K. On the liquid side, the GT model overpredicts the saturated liquid density at high temperatures, while underpredicting the saturated liquid density at low temperatures when compared to experiment. The critical parameters are well reproduced by the TraPPE model [experimental values in brackets, taken from NIST (2000)]: $T_c = 126.5$ K (126.19 K), $P_c = 34.6$ bar (33.98 bar), $\rho_c = 308.0$ kg/m^3 (313.11 kg/m^3).

Mixtures

As a further test of our models for CO_2 and N_2, we performed calculations for a number of binary mixtures. The first of these mixtures was CO_2/propane at $T = 294.15$ K, which was also used in the parametrization of the TraPPE CO_2 model (see earlier). In Figure 5, the results of the simulations for the TraPPE force field are shown. For comparison, we also include results for simulations of the EMP2 CO_2 model (Harris and Yung, 1995) with the TraPPE-EH propane model and the experimental data of Reamer et al. (1951). As an

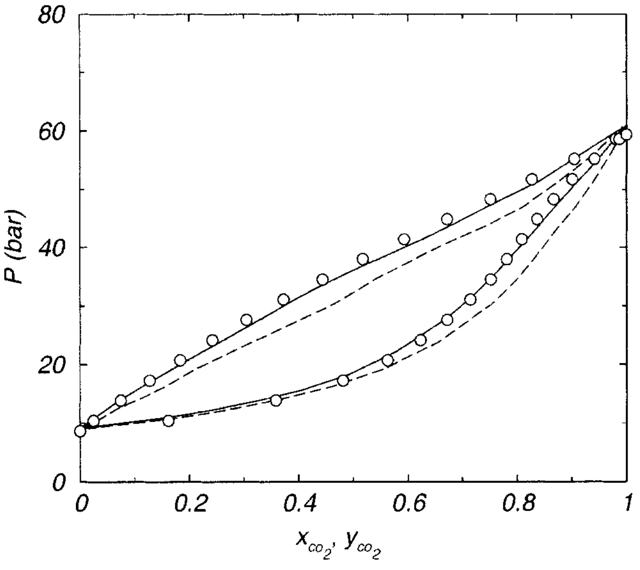

Figure 5. Pressure-composition diagram for CO_2/propane at 294.15 K.

Experimental data (circles) (Reamer et al., 1951), EMP2/TraPPE-EH propane (dashed line), TraPPE CO_2/TraPPE-EH propane (solid line).

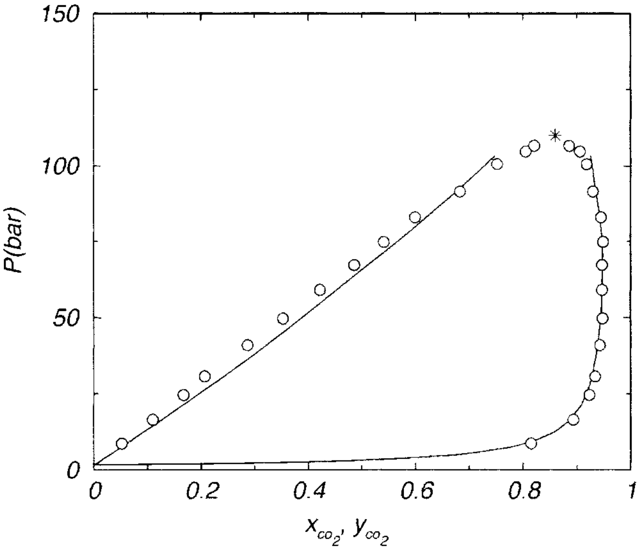

Figure 6. Pressure-composition diagram for CO_2/n-hexane at 353.15 K.

Experimental data (circles) (Li et al., 1981) and TraPPE CO_2/TraPPE-EH n-hexane (solid line and asterisk).

aside, it should be noted here that the data of Reamer et al. are valid only below the critical temperature of CO_2 (Niesen and Rainwater, 1990). The combination of the EMP2/TraPPE-EH force fields is only in qualitative agreement with experiment, and exhibits significant deviations from the experimental data for both the liquid and vapor phases. These deviations become increasingly severe as the concentration of CO_2 in the system increases. Simulation results for the TraPPE CO_2/TraPPE-EH propane force fields, on the other hand, are in good agreement with experiment over the entire composition range. Only slight deviations from experiment are found in the liquid phase.

Another area of concern in the development of intermolecular force fields is that of transferability. The parameters for the TraPPE CO_2 force field were originally tuned to improve the CO_2/propane binary-mixture phase behavior while retaining the correct pure-component phase behavior of the EMP2 force field. If the model is "transferable," then it should yield phase behavior that is quantitatively in agreement with experiment for any CO_2/n-alkane mixture. As an example of this, simulations were performed for TraPPE CO_2/TraPPE-EH n-hexane. The pressure-composition diagram for this system at 353.15 K is presented in Figure 6. Over the entire composition range, the simulation data are in good agreement with the experimental data of Li et al. (1981). Only small deviations are present in the liquid phase, which is consistent with the observations made for the CO_2/propane system. In addition, the estimated critical parameters of $P_c = 109.9$ bar and $x_c^{CO_2} = 0.86$ agree rather well with their experimental counterparts of $P_c = 108.3$ bar and $x_c^{CO_2} = 0.85$ (Li et al., 1981; Choi and Yeo, 1998). These results are a significant improvement over those of a recent Gibbs ensemble study of CO_2/n-hexane mixtures by Cui et al. (1999) where united-atom alkane models were used.

Simulations for binary mixtures containing N_2 were also performed. Because the pure-component results for the vapor pressure of the GT force field showed significant deviations from experiment, calculations were only performed for the TraPPE force field. In Figure 7, the pressure-composition diagram for CO_2/N_2 at 253.15 K is shown. The simulation results are in good agreement with the experimental measurements (Gmehling and Onken, 1977) for the vapor compositions, but the solubility of N_2 in liquid CO_2 is underestimated slightly. The temperature used here is nearly twice the critical temperature of N_2, and we speculate that the functional form of the simple LJ potential can lead to inaccuracies at these high reduced temperatures. Critical parameters for this mixture were estimated from a mixed-field analysis to be $P_c = 160.2$ bar and $x_c^{CO_2} = 0.612$. Corresponding experimental critical-point data are not availible.

The last of the binary mixtures studied was TraPPE N_2/TraPPE-EH propane. In Figure 8, the pressure-composition diagram for N_2/propane at 270 K is shown along with the experimental results of Yucelen and Kidnay (1999). In the liquid phase, the simulation and experimental data are in good agreement. The simulation results show small deviations from experiment in the vapor phase, as the solubility of N_2 in liquid propane is underpredicted slightly. The estimated critical parameters are $P_c = 185.2$ bar and $x_c^{N_2} = 0.626$. As in the case of the CO_2/N_2 mixture, the corresponding experimental critical parameters could not be found.

We complete our study by presenting the phase diagram for the ternary mixture of CO_2/N_2/propane at 270 K and 60 bar in Figure 9. The simulation data are in good agreement with experiment (Yuculen and Kidnay, 1999) for both the liquid and vapor phases, demonstrating the predictive power of molecular simulation given an accurate and consistent set of intermolecular force fields. The reader is reminded that in this work the Lorentz-Berthelot combining rules were used for *all* unlike LJ interactions, and no special binary interaction parameters were necessary to achieve quantitative agree-

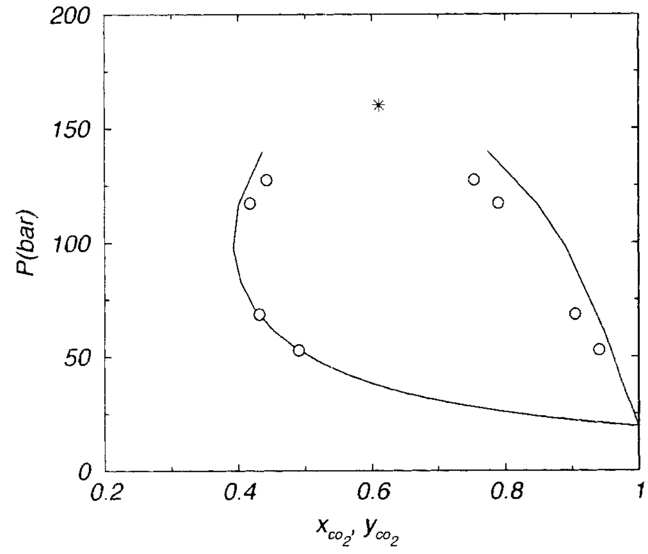

Figure 7. Pressure-composition diagram for CO_2/N_2 at 253.15 K.

Experimental data (circles) (Gmehling and Onken, 1977) and TraPPE CO_2/TraPPE N_2 (solid line and asterisk).

ment with experiment. This is a significant advance over other recent studies of mixture-phase behavior via molecular simulation, which have used special combining rules for unlike-pair interactions belonging to interaction sites on molecules of different types (Potoff et al., 1999) or have fitted system-specific binary interaction parameters (Vrabec and Fischer, 1997; Liu and Beck, 1998).

Conclusions

In this work we have developed the TraPPE force fields for CO_2 and N_2. These models were found to reproduce experimental results for the pure components to a high accuracy. For mixtures containing CO_2, our new model was found to yield results that are in quantitative agreement with experiment, while previous simulations for CO_2/alkane mixtures were not able to predict the correct phase behavior when Lorentz-Berthelot combining rules were consistently used. Our CO_2 model was shown to be transferable, in the sense that the phase behavior of CO_2/propane and CO_2/*n*-hexane are equally well reproduced. Simulations of mixtures of CO_2/N_2, however, showed small, but noticeable deviations from experiment. As a result, further refinements might be necessary for the N_2 force field, the most likely being the addition of a third Lennard-Jones site at the bond center to better tune the dispersive interactions and the repulsive shape of the model. Finally, with the calculation of the ternary phase diagram for CO_2/N_2/propane, we have shown that molecular simulation can be used to predict the phase behavior of complex, multicomponent systems to a high accuracy without requiring special binary interaction parameters.

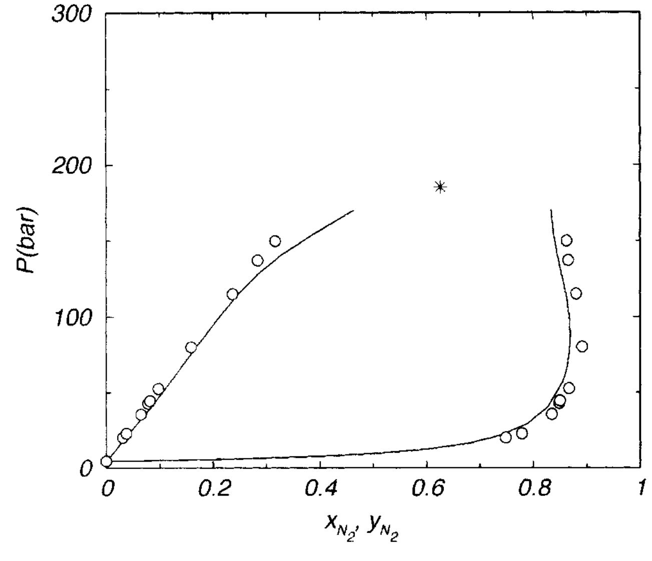

Figure 8. Pressure-composition diagram for N_2/propane at 270 K.

Experimental data (circles) (Yucelen and Kidnay, 1999) and TraPPE CO_2/TraPPE N_2 (solid line and asterisk).

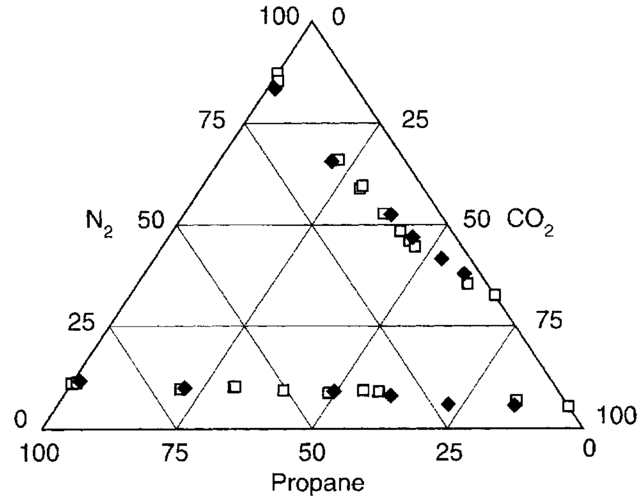

Figure 9. Ternary phase diagram for CO_2/N_2/propane at 270 K and 60 bar.

Experimental data (squares) (Yucelen and Kidnay, 1999) and TraPPE CO_2/TraPPE N_2/TraPPE-EH propane (diamonds).

Acknowledgments

Financial support from the National Science Foundation, an Alfred P. Sloan Research Fellowship, and an MSI Research Scholarship (J.J.P.) is gratefully acknowledged. Part of the computer resources were provided by the Minnesota Supercomputing Institute (MSI). We thank Bin Chen for stimulating discussions.

Literature Cited

Allen, M. P., and D. J. Tildesley, *Computer Simulation of Liquids*, Clarendon Press, Oxford (1987).

Baranyai, A., and P. T. Cummings, "Liquid-Vapor Coexistence by Molecular Dynamics Simulation," *J. Chem. Phys.*, **112**, 3516 (2000).

Bruce, A. D., and N. B. Wilding, "Scaling Fields and Universality of the Liquid-Gas Critical Point," *Phys. Rev. Lett.*, **68**, 193 (1992).

Brunner, G., *Gas Extraction*, Springer, New York (1991).

Chen, B., and J. I. Siepmann, "Transferable Potentials for Phase Equilibria: 3. Explicit-Hydrogen Description of Normal Alkanes," *J. Phys. Chem. B*, **103**, 5370 (1999).

Choi, E-J., and S-D. Yeo, "Critical Properites for Carbon Dioxide + n-Alkane Mixtures Using a Variable-Volume View Cell," *J. Chem. Eng. Data*, **43**, 714 (1998).}

Cui, S. T., H. D. Cochran, and P. T. Cummings, "Vapor-Liquid Phase Coexistence of Alkane-Carbon Dioxide and Perfluoroalkane-Carbon Dioxide Mixtures," *J. Phys. Chem. B*, **103**, 4485 (1999).

Ferrenberg, A. M., and R. H. Swendsen, "New Monte Carlo Technique for Studying Phase Transitions," *Phys. Rev. Lett.*, **61**, 2635 (1988).

Ferrenberg, A. M., and R. H. Swendsen, "Optimized Monte Carlo Data Analysis," *Phys. Rev. Lett.*, **63**, 1195 (1989).

Galassi, G., and D. J. Tildesley, "Phase Diagrams of Diatomic Molecules Using the Gibbs Ensemble Monte Carlo Method," *Mol. Simp.*, **13**, 11 (1994).

Gmehling, J., and U. Onken, *Vapor-Liquid Equilibrium Data Collection*, Scholium International, Flushing, NY (1977).

Gray, C. G., and K. E. Gubbins, *Theory of Molecular Fluids*, Vol. 1, *Fundamentals*, Clarendon Press, Oxford (1984).

Harris, J. G., and K. H. Yung, "Carbon Dioxide's Liquid-Vapor Coexistence Curve and Critical Properties as Predicted by a Simple Molecular Model," *J. Phys. Chem. B*, **99**, 12021 (1995).

Jorgensen, W. L., J. Chandrasekhar, J. D. Madura, R. W. Impey, and M. L. Klein, "Comparison of Simple Potential Functions for Simulating Liquid Water." *J. Chem. Phys.*, **79**, 926 (1983).

Kofke, D. A., "Direct Evaluation of Phase Coexistence by Molecular Simulation via Integration Along the Saturation Line," *J. Chem. Phys.*, **98**, 4199 (1992).

Kong, C. L., "Combining Rules for Intermolecular Potential Parameters: II. Rules for the Lennard-Jones (12-6) Potential and the Morse Potential," *J. Chem. Phys.*, **59**, 2464 (1973).

Li, Y.-H., K. H. Dillard, and R. L. Robinson Jr., "Vapor-Liquid Phase Equilibrium for Carbon Dioxide-n-Hexane at 40, 80, and 120°C," *J. Chem. Eng. Data*, **26**, 53 (1981).

Liu, A., and T. L. Beck, "Vapor-Liquid Equilibria of Binary and Ternary Mixtures Containing Methane, Ethane, and Carbon Dioxide from Gibbs Ensemble Simulations," *J. Phys. Chem. B*, **102**, 7627 (1998).

Maitland, G. C., M. Rigby, E. B. Smith, and W. A. Wakeham, *Intermolecular Forces: Their Origin and Determination*, Clarendon Press, Oxford (1981).

Martin, M. G., and J. I. Siepmann, "Novel Configurational-Bias Monte Carlo Method for Branched Molecules. Transferable Potentials for Phase Equilibria: 2. United-Atom Description of Branched Alkanes," *J. Phys. Chem. B*, **103**, 973 (1999).

Mishima, K., K. Matsuyama, D. Tanabe, S. Yamauchi, T. J. Young, and K. P. Johnston, "Microencapsulation of Proteins by Rapid Expansion of Supercritical Solution with a Nonsolvent," *AIChE J.*, **46**, 857 (2000).

Moldover, R. M., and J. S. Gallagher, "Critical Points of Mixtures: An Analogy with Pure Fluids," *AICHE J.*, **24**, 267 (1978).

Murthy, C. S., S. F. O'Shea, and I. R. McDonald, "Electrostatic Interactions in Molecular Crystals. Lattice Dynamics of Solid Nitrogen and Carbon Dioxide," *Molec. Phys.* **50**, 531 (1983).

Niesen, V. G., and J. C. Rainwater, "Critical Locus, (Vapor + Liquid) Equilibria, and Coexisting Densities of (Carbon Dioxide + Propane) at Temperatures from 311 K to 361 K," *J. Chem. Thermodyn.*, **22**, 777 (1990).

NIST Chemistry WebBook, available on the Web at http://webbook.nist.gov/chemistry/(2000).

Panagiotopoulos, A. Z., "Direct Determination of Phase Coexistence Properties of Fluids by Monte Carlo Simulation in a New Ensemble," *Molec. Phys.*, **61**, 813 (1987).

Panagiotopoulos, A. Z., N. Quirke, M. Stapleton, and D. J. Tildesley, "Phase Equlibria by Simulation in the Gibbs Ensemble. Alternative Derivation, Generalization and Application to Mixture and Membrane Equilibria," *Mol. Phys.*, **63**, 527 (1988).

Potoff, J. J., and A. Z. Panagiotopoulos, "Critical Point and Phase Behavior of the Pure Fluid and a Lennard-Jones Mixture," *J. Chem. Phys.*, **109**, 10914 (1998).

Potoff, J. J, J. R. Errington, and A. Z. Panagiotopoulos, "Molecular Simulation of Phase Equilibria for Mixtures of Polar and Non-Polar Components," *Mol. Phys.*, **97**, 1073 (1999).

Rainwater, J. C., *Supercritical Fluid Science and Technology*, T. J. Bruno and J. F. Ely, eds., CRC Press, Ann Arbor, MI (1991).

Reamer, H. H., B. H. Sage, and W. N. Lacey, "Phase Equilibria in Hydrocarbon Systems: Volumetric Phase Behavior of the Propane-Carbon Dioxide System," Ind. Eng. Chem., **43**, 2515 (1951).

Reid, R. C., J. M. Prausnitz, and T. K. Sherwood, *The Properties of Gases and Liquids*, McGraw-Hill, New York (1977).

Vrabec, J., and J. Fischer, "Vapor-Liquid Equilibria of the Ternary Mixture $CH_4 + C_2H_6 + CO_2$ from Molecular Simulation," *AIChE J.*, **43**, 212 (1997).

Wilding, N. B., "Critcal-Point and Coexistence-Curve Properties of the Lennard-Jones Fluid: A Finite-Size Scaling Study," Phys. Rev. E, **52**, 602 (1995).

Yucelen, B., and A. J. Kidnay, "Vapor-Liquid Equilibria in the Nitrogen + Carbon Dioxide + Propane System from 240 to 330 K at Pressures to 15 MPa," *J. Chem. Eng. Data.*, **44**, 926 (1999).

Manuscript received June 26, 2000, and revision received Feb. 28, 2001.